An adaptive ALE residual based penalization approach for laminar flows with moving bodies

Leo Nouveau, Heloise Beaugendre, M Ricchiuto, Cecile Dobrzynski, Rémi Abgrall

An adaptive ALE residual based penalization approach for laminar flows with moving bodies

L. Nouveau, H. Beaugendre , M. Ricchiuto, C. Dobrzynski, R. Abgrall

RESEARCH REPORT
N° 8936
Juillet 2016
Project-Team Cardamom

ISSN 0249-6399 ISRN INRIA/RR--8936--FR+ENG

An adaptive ALE residual based penalization approach for laminar flows with moving bodies

L. Nouveau*, H. Beaugendre† *, M. Ricchiuto*,
C. Dobrzynski*†, R. Abgrall‡

Project-Team Cardamom

Research Report n° 8936 — Juillet 2016 — 15 pages

Abstract: The coupling of anisotropic unstructured mesh adaptation techniques with an immersed boundary method (IBM) called penalization is studied for time dependent flow simulations involving moving objects. To extend Residual Distribution (RD) method to the penalized Navier Stokes equations, a new formulation based on a Strang splitting is developed. To reduce the error on solid boundaries, unstructured mesh adaptation based on an elasticity model is used. Keeping a constant connectivity, the mesh evolves in time according to the solid position, and the new formulation is proposed in an ALE framework.

Key-words: Penalization, Residual Distribution Schemes, mesh adaptation, ALE

* Inria BSO, Team Cardamom
† Bordeaux INP, IMB UMR 5251
‡ Institute of Mathematics & Computational Science, Zürich University

RESEARCH CENTRE
BORDEAUX – SUD-OUEST

351, Cours de la Libération
Bâtiment A 29
33405 Talence Cedex

Méthode de pénalization basée sur une approche d'adaptation en formalisme résidu distribué ALE pour des objets mobiles en écoulement laminaire

Résumé : Le couplage des techniques d'adaptation de maillages non structurés anisotropes avec une méthode de frontière immergée (IBM) appelée Pénalization est étudié pour des simulations instationnaires impliquant des objents en mouvement. Pour étendre les méthodes de distribution du résidu (RD) aux équations de Navier Stokes pénalisées, une nouvelle formulation basée sur un splitting de Strang est développée. Pour réduire l'erreur sur les frontières du solide, une adaptation de maillage non structuré est utilisée, basée sur un modèle d'élasticité. Gardant une connectivité constante, le maillage évolue en temps en accord avec la position du solide, et la nouvelle formulation est proposée dans un formalisme ALE.

Mots-clés : Pénalisation, Schémas au résidu distribué, Adaptation de maillage, ALE.

1 Introduction

The interest on Immersed Boundary Methods is increasing in Computational Fluid Dynamics as they simplify the mesh generation problem. In particular, the generation of efficient and valid meshes for moving bodies may become difficult. The starting point of this work is an IBM known as penalization introduced by Brinkmann in 1947 for a swarm of particles [1]. A source term is added to the Navier Stokes equations to account for the forces exchanged between the fluid and the solid [2]. To adapt RD schemes to the IBM considered, we have proposed a new formulation based on a Strang splitting method in time [3]. This splitting couples an implicit asymptotic integration procedure of the penalized ordinary differential equation with a RD scheme for the Navier-Stokes equations [4]. The aim is to deal with moving bodies. As we want to reduce the error on the solid definition, mesh adaptation is performed, based on an elasticity model (see for instance [5]) conserving the mesh connectivity. Thus, this new formulation is proposed in the ALE framework, avoiding interpolation steps, as required in other approaches based on remeshing (see for instance [6] or [7]).

2 Problem Statement

Immersed boundary methods are characterized by a mesh covering the entire domain. The first step is then to locate the position of a solid on the mesh $\mathcal{T}_h$ of the domain Ω. A common way to perform this, is to use a level set function which gives the distance from any point of the mesh to the closest solid boundary. We will use the *signed distance function* (SDF) as a level set function.

2.1 Signed Distance Function

The SDF ψ of a point is the distance of the considered point to the solid surface with a sign in order to determine if the point is inside or outside the solid. We choose, as a convention, that for an inside point, the SDF is negative and for an outside one, the SDF is positive. Thus, the inside of a solid is characterised by Ω:

$$\Omega = \{x \in \mathbb{R}^d \mid \psi_0(x) < 0\} \text{ and } \partial\Omega = \{x \in \mathbb{R}^d \mid \psi_0(x) = 0\} \tag{1}$$

with d the dimension of space and ψ_0 a continuous function.
The SDF can be computed as the solution of the following *unsteady Eikonal equation :*

$$\begin{cases} \partial_t \psi + sgn(\psi_0)(||\nabla\psi|| - 1) = 0 \ \forall t > 0, \ x \in \mathbb{R}^d \\ \psi(t = 0, x) = \psi_0(x), \ \forall x \in \mathbb{R}^d \end{cases} \tag{2}$$

One way to solve (2) is to use the method of characteristics (as proposed by Dapogny and Frey in [8]). Once the SDF is defined all over the domain for a solid S, the characteristic function χ_S of the solid can be defined as:

$$\begin{cases} \chi_S = 1, \text{ inside } S \\ \chi_S = 0, \text{ outside } S \end{cases} \tag{3}$$

2.2 Penalization and residual based, splitting approach

We consider the penalized Navier Stokes system of equations :

$$\partial_t \mathbf{u} + \nabla \cdot \mathbf{F}(\mathbf{u}) - \nabla \cdot \mathbf{G}(\mathbf{u}, \nabla\mathbf{u}) + \mathbf{S}(\mathbf{u}) = 0 \tag{4}$$

where $\mathbf{u}$ is the vector of unknowns in conservative form, $\mathbf{F}$ and $\mathbf{G}$ are the advective and viscous flux, and $\mathbf{S}$ is the penalty term. They are defined as follows:

$$\mathbf{u} = \begin{pmatrix} \rho \\ \rho\mathbf{v} \\ \rho e \end{pmatrix} \qquad \mathbf{F}(\mathbf{u}) = \begin{pmatrix} \rho\mathbf{v} \\ \rho\mathbf{v} \otimes \mathbf{v} + p\underline{\mathbf{Id}} \\ (\rho e + p)\mathbf{v} \end{pmatrix} \qquad \mathbf{G} = \begin{pmatrix} 0 \\ \underline{\boldsymbol{\pi}} \\ \underline{\boldsymbol{\pi}}\mathbf{v} + \mathbf{q} \end{pmatrix}$$
$$\mathbf{S} = \frac{1}{\eta}\chi_S \begin{pmatrix} 0 \\ \rho(\mathbf{v} - \mathbf{v}_S) \\ \theta_S \rho(\epsilon_{int} - \epsilon_{intS}) + \rho(\mathbf{v} - \mathbf{v}_S)\mathbf{v} \end{pmatrix} \tag{5}$$

where ρ is the density, $\mathbf{v}$ the velocity vector, e the total energy, ϵ_{int} the internal energy, p the pressure, $\underline{\pi}$ is the stress tensor and $\mathbf{q}$ the heat flux. In addition of these equations, the variables are linked by an equation of state, in our case, we consider the perfect gas law. Inside the penalty source term, η is the penalty parameter ($\eta \sim 10^{-10}$), χ_S the characteristic function of the solid and $\mathbf{u}_S$ the vector of penalized values we want to impose inside the solid. θ_S lets the possibility to penalize the energy (Dirichlet BC) or not (Neumann BC).

This system of unsteady equations will be solved using a residual distribution scheme (see [9, 10, 11] for steady problems and [12, 13, 14] for unsteady ones). Starting from the explicit second order Runge Kutta (RK2) scheme proposed by Ricchiuto *et al.* [12, 13], a Strang Splitting [3] is performed to solve implicitly the penalty source term as proposed by the authors for motionless bodies in [4]. The basic idea of a splitting is to solve (4) by part :

$$\begin{cases} \partial_t \mathbf{u} + \nabla \cdot \mathbf{F}(\mathbf{u}) - \nabla \cdot \mathbf{G}(\mathbf{u}, \nabla \mathbf{u}) = 0 \\ \partial_t \mathbf{u} + \mathbf{S}(\mathbf{u}) = 0 \end{cases} \tag{6}$$

The first part of (6) consists in solving the classical Navier Stokes equations, and the second part accounts for the penalty term. Let $S_{(NS,\Delta t)}$ be the operator, second order in space and time, used to solve the NS part of the equations and $S_{(P,\Delta t)}$ the operator used to solve the penalty part, those two operators being second order accurate in time. To conserve a second order in space and time, the Strang splitting is summarized as follows:

$$\begin{cases} \overline{\mathbf{u}}^{n+\frac{1}{2}} = S_{(P,\frac{\Delta t}{2})} \mathbf{u}^n \\ \mathbf{u}^{n+\frac{1}{2}} = S_{(NS,\Delta t)} \overline{\mathbf{u}}^{n+\frac{1}{2}} \\ \mathbf{u}^{n+1} = S_{(P,\frac{\Delta t}{2})} \mathbf{u}^{n+\frac{1}{2}} \mathbf{u}^{n+\frac{1}{2}} \end{cases} \tag{7}$$

In the setting of penalization, the second part of (6) leads to the resolution of an Ordinary Differential Equations (ODE). In this case, the operator $S_{(P,\Delta t)}$ is chosen to be a truncation with error in η^2 of the asymptotic approximation of the solution, see [4] (we recall that η is a very small parameter $\approx 10^{-10}$ in our simulations) :

$$S_{(P,\frac{\Delta t}{2})} \mathbf{u}(t_0) = \mathbf{u}(t_0) e^{-\frac{\Delta t}{2\eta}} + (\eta \partial_t \mathbf{u}_S(t_0) - \mathbf{u}_S(t_0)) e^{-\frac{\Delta t}{2\eta}} + \mathbf{u}_S(t_0 + \frac{\Delta t}{2}) - \eta \partial_t \mathbf{u}_S(t_0 + \frac{\Delta t}{2}) \tag{8}$$

where $\mathbf{u}(t_0) = \mathbf{u}^n$ for the first step of (7) and $\mathbf{u}(t_0) = \mathbf{u}^{n+\frac{1}{2}}$ for the last one. This process guarantees a global second order accuracy in space and time for explicit discretization of the interface. In the proposed approach, the accuracy of the BC imposition is recovered using mesh adaptation, without claiming second order accuracy.

3 An elasticity model for mesh adaptation

3.1 The Elasticity Model, Referential and Adapted Mesh

Mesh adaptation close to solid boundaries is used to increase the definition of the solid geometry. However, as the solid is moving (or moved by the flow), the adaptation has to be unsteady. As explained previously, the aim here is to solve the equations over an ALE formulation with r-adaptation [5, 15, 16, 17, 18]. So as to reach this purpose, the mesh will be assimilated to an elastic material (such as proposed in [15]) constrained by a force. In our study, this force is defined so as to refine the mesh around the 0 isovalue of the SDF ψ and to chosen physical parameters.
From now on, the following notations will be used : $\boldsymbol{\chi} = (\chi, \eta)$ will denote the coordinates into the fixed referential domain and $\boldsymbol{x} = (x, y)$ the coordinates in the adapted one. Thus the elasticity equation ruling the adaptation writes :

$$\boldsymbol{\nabla}_{\boldsymbol{\chi}} . \underline{\boldsymbol{\sigma}}(\underline{\boldsymbol{\epsilon}}(\mathbf{u})) = \mathbf{F} \tag{9}$$

where $\mathbf{u} = (\mathbf{u}_x, \mathbf{u}_y)^T$ is the deformation ($u_{x,i} = x_i - \chi_i, u_{y,i} = y_i - \eta_i$), $\underline{\boldsymbol{\epsilon}}(\mathbf{u}) = \frac{1}{2}(\boldsymbol{\nabla}_{\boldsymbol{\chi}} \mathbf{u} + (\boldsymbol{\nabla}_{\boldsymbol{\chi}} \mathbf{u})^T)$ is the tensor of deformation and $\underline{\boldsymbol{\sigma}} = \lambda tr(\underline{\boldsymbol{\epsilon}}) + 2\mu \underline{\boldsymbol{\epsilon}}$ is the stress tensor, with λ, μ the Lamé coefficients. The aim is to properly defined the force F according to the wanted adaptation. In our case, F is chosen to depend on the gradient of a *monitor function* ω (inspired from mesh adaptation proposed in [16, 17, 18, 5] among others). This monitor function depends on the SDF ψ and the physical variable v as :

$$\begin{cases} \mathbf{F}_x = \partial_\chi \omega, \mathbf{F}_y = \partial_\eta \omega \\ \omega = \max(\omega_\psi, \omega_v) \\ \omega_\psi = \sqrt{\alpha_\psi e^{-\beta\psi^2}}, \qquad \omega_v = \sqrt{\alpha_v \dfrac{||\boldsymbol{\nabla} v||}{\gamma ||\boldsymbol{\nabla} v||_{max}}} \end{cases} \tag{10}$$

α_ψ and α_v are coefficients allowing to moderate the SDF and physical adaptations. β allows to control the width of refinement around the 0 isovalue of ψ and γ allows to normalize the gradient of the physical solution. For the computations, it has been set for the Lamé coefficients : $\lambda = E\nu/((1+\nu)(1-2\nu))$ and $\mu = E/(2(1+\nu))$, with $E = 1$, $\nu = 0.45$
To solve this problem (9,10), a finite element discretization is employed with a Newton Gauss Seidel algorithm. This is the subject of the next section.

3.2 Finite Element Resolution

Let rewrite properly the problem with the corresponding boundary conditions :

$$\begin{cases} \boldsymbol{\nabla}_{\boldsymbol{\chi}}.\underline{\boldsymbol{\sigma}}(\underline{\boldsymbol{\epsilon}}(\mathbf{u})) = \mathbf{F} & \text{on } \Omega_{\boldsymbol{\chi}} \quad (11) \\ \mathbf{u} = \mathbf{0} & \text{on } \partial\Omega_{\boldsymbol{\chi}} \quad (12) \end{cases}$$

The boundary condition (12) is chosen to keep the mesh fixed on the boundary of the domain. The weak formulation writes, considering a test function $\boldsymbol{w} = (w_x, w_y) \in [H_0^1]^2$, find $\mathbf{u} \in [H_0^1]^2$ such that :

$$\int_\Omega \underline{\boldsymbol{\epsilon}}(\boldsymbol{w}) : \underline{\boldsymbol{\sigma}}(\boldsymbol{u}) = \int_\Omega \mathbf{F}.\boldsymbol{w}, \qquad \forall \boldsymbol{w} \in [H_1^0]^2 \tag{13}$$

where $\underline{\mathbf{A}} : \underline{\mathbf{B}} = \sum_i \sum_j A_{ij} B_{ji}$ is the double dot product.
Let consider a triangulation $\mathcal{T}^h$ of the domain, whom elements are denoted T with boundaries ∂T and area $|T|$, we set $u_{x/y} = \sum_{j \in T_\chi} u_{x/y,j} \varphi_j$ the approximated solution, φ_j being the j^{th} 2^{nd} order Lagrange basis function.This problem (13) is then discretized with FE over the classical way :

$$\underline{\boldsymbol{\mathcal{K}}}\mathbf{U} = \underline{\mathbf{M}}\mathbf{F}$$
$$\underline{\boldsymbol{\mathcal{K}}} = \begin{pmatrix} \underline{\boldsymbol{\mathcal{K}}}_1 & \underline{\boldsymbol{\mathcal{K}}}_2 \\ \underline{\boldsymbol{\mathcal{K}}}_3 & \underline{\boldsymbol{\mathcal{K}}}_4 \end{pmatrix}, \mathbf{U} = \begin{pmatrix} \mathbf{U}_x \\ \mathbf{U}_y \end{pmatrix}, \underline{\mathbf{M}} = \begin{pmatrix} \underline{\mathbf{M}}^{Gal} & \mathbf{0} \\ \mathbf{0} & \underline{\mathbf{M}}^{Gal} \end{pmatrix}, \mathbf{F} = \begin{pmatrix} \mathbf{F}_x \\ \mathbf{F}_y \end{pmatrix} \tag{14}$$

where $\mathbf{U}_x$, $\mathbf{U}_y$ are the vector of the x and y displacements, $\underline{\mathbf{M}}^{Gal}$ is the Galerkin mass matrix :

$$(\underline{\mathbf{M}}^{Gal})_{ij} = \sum_{T \ni i} \sum_{j \in T} \varphi_i \varphi_j = \begin{cases} \displaystyle\sum_{T \ni i} \frac{|T|}{6}, & \text{if } i = j \\ \displaystyle\sum_{T \ni i} \frac{|T|}{12}, & \text{if } i \neq j \end{cases} \tag{15}$$

and the $\underline{\boldsymbol{\mathcal{K}}}_{\alpha,\alpha=1,2,3,4}$ are defined by :

$$(\underline{\boldsymbol{\mathcal{K}}}_\alpha)_{ij} = \sum_{T \ni i} \sum_{j \in T} \frac{1}{4|T|} \left[\underline{\boldsymbol{\mathcal{M}}}_\alpha \mathbf{n}_j\right] .\mathbf{n}_i \tag{16}$$

where $\mathbf{n}_i$ is the inward normal on the opposite edge of node i.
Remark : Those matrices are defined on the **reference mesh** : they only need to be evaluated at the beginning of the computation.
However, in the RHS, the forces depends on the adapted mesh. Indeed, coming back on its definition :

$$\mathbf{F}_x = \partial_\chi \omega(\boldsymbol{x}) \qquad \mathbf{F} = \partial_\eta \omega(\boldsymbol{x}) \tag{17}$$

the notation $\boldsymbol{x}$ stands for the nodal coordinates of the adapted mesh. Thus, following the idea proposed in [16] or [19], a limited number of Newton Gauss Seidel process (10 for the proposed work) is performed at each time step , with as initial condition the position of the nodes at time t^n. Indeed, as the solution

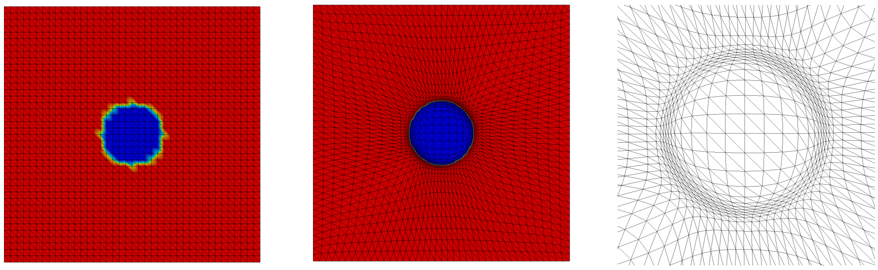

Figure 1: Adaptation to a circle level set function. Left : Referential mesh and 0 level set function - Middle : Adapted mesh and 0 level set function - Right : Zoom close to the refined area

is not supposed to evolve a lot during one time step, the initial solution is closed to the converged one. So as to briefly illustrate this method in the present section, an adaptation to a circle is proposed figure 1.

As the connectivity is kept constant all over the time, this elasticity model is well suited to combine with an ALE formulation of our physical problem. The following section presents the ALE RD scheme used to solve our penalized Navier Stokes equations for moving bodies. Recall that ALE formulation avoids interpolations steps.

4 ALE RD scheme

In this section, we briefly give the tools to construct RD schemes. Some general notions for dealing with unsteady problems are introduced before giving its extension proposed in [19] for the ALE framework.

4.1 Unsteady Conservation Law and RD Schemes

For simplicity, we present the schemes for the 2D scalar advection-diffusion equation :

$$\frac{\partial u}{\partial t} + \boldsymbol{\nabla} \cdot \boldsymbol{\mathcal{F}}(u) = \boldsymbol{\nabla} \cdot (\nu \boldsymbol{\nabla} u), \quad \text{on } \Omega \tag{18}$$

Given a triangulation $\mathcal{T}^h$ of Ω, elements denoted T of boundaries ∂T and area $|T|$, the approximated solution is defined as $u_h(x, y, t) = \sum_i u_i^n \varphi_i(x, y)$, $u_i^n = u_h(x_i, y_i, t^n)$, where φ_i are the Lagrange basis function. We denote by $\mathbf{a}$ the wave speed obtained as the Jacobian of the flux : $\mathbf{a} = \boldsymbol{\nabla}_u \boldsymbol{\mathcal{F}}$.
The first step is to define for each triangle the *total residual* as :

$$\Phi^T(u_h) = \int_T [\partial_t u_h + \mathbf{a} \cdot \boldsymbol{\nabla} u_h - \boldsymbol{\nabla} \cdot (\nu \boldsymbol{\nabla} u_h)] = \int_T \partial_t u_h + \phi^T(u_h) \tag{19}$$

where $\phi^T(u_h)$ is called the *fluctuation*.
The principle of a RD scheme is to distribute this residual to the degree of freedom (DoF) using *distribution coefficient* β_i^T (in our study, the DoF are only the nodes, for second order accuracy) and to sum for each DoF the contribution of the surrounding elements that must be null [10, 11, 13, 20, 21]. In the present study, the explicit second order RK scheme proposed by some of the authors in [12, 13] is employed. The use of mass lumping and the time shifted operator presented in the above references lead to the fully explicit scheme :

$$\begin{cases} |C_i| \dfrac{u_i^* - u_i^n}{\Delta t} + \displaystyle\sum_{T \ni i} \phi_i^T(u_h^n) = 0 \\ |C_i| \dfrac{u_i^{n+1} - u_i^*}{\Delta t} + \displaystyle\sum_{T \ni i} \left(\beta_i^T \int_T \frac{u_i^* - u_i^n}{\Delta t} + \frac{1}{2}(\phi_i^T(u_h^*) + \phi_i^T(u_h^n)) \right) = 0 \end{cases} \tag{20}$$

The $\phi_i^T(u_h)$ are called *nodal fluctuation* and are defined by :

$$\phi_i^T(u_h) = \beta_i^T \phi^T(u_h) \tag{21}$$

However, for the case of advection diffusion problems, they are slightly modified so as to recover full second order accuracy as proposed in [11] making the use of a gradient recovery technique. Denoting the reconstructed gradient by $\widetilde{\nabla u_h}$, it modifies them as follows :

$$\phi_i^T(u_h) = \beta_i^T \phi^T(u_h) + \int_T \nu \nabla\varphi_i \cdot (\nabla u_h - \widetilde{\nabla u_h}) \tag{22}$$

The fluctuation being computed with the reconstructed gradient. For the simulations that will be presented later on, the SUPG scheme is used, defined by the distribution coefficients :

$$\beta_i^T = \frac{1}{3} + k_i\tau, \qquad k_i = \frac{1}{2}\bar{\mathbf{a}}.\mathbf{n}_i, \qquad \tau = \left(\sum_{j\in T} |k_j| + \nu\right)^{-1} \tag{23}$$

where $\bar{\mathbf{a}} = \sum_{j\in T} \frac{\mathbf{a}_j}{3}$.
The extension to the compressible Navier Stokes system of equations has been fully developed in [21] for the steady case and adapted to the unsteady ones in [4]. The nodal fluctuations are defined (using notations proposed in equation (5)) :

$$\boldsymbol{\phi}_i^T(\mathbf{u}_h) = \frac{\boldsymbol{\phi}^T(\mathbf{u}_h)}{3} + \int_T \mathbf{A}\cdot\nabla\varphi_i \boldsymbol{\tau}(\mathbf{A}\cdot\nabla\mathbf{u}_h - \nabla\cdot(\mathbf{K}(\mathbf{u}_h)\widetilde{\nabla\mathbf{u}_h})) + \int_T \mathbf{K}(\mathbf{u}_h)\nabla\varphi_i\cdot(\nabla u_h - \widetilde{\nabla\mathbf{u}_h}) \tag{24}$$

where $\mathbf{A}$ is the Jacobian of the Euler flux $\mathbf{F}$ and $\mathbf{K}$ is defined such that the viscous flux writes $\mathbf{G} = \mathbf{K}\nabla\mathbf{u}_h$, and the stabilization matrix $\boldsymbol{\tau}$ is defined by :

$$\boldsymbol{\tau} = \frac{1}{3}\left(\sum_{i\in T}[|\mathbf{A}| + \mathbf{K}]\right)^{-1} \tag{25}$$

4.2 RD schemes in an ALE framework

It is now briefly explained how the previous RK2 scheme is adapted to the ALE framework. Considering the computational domain $\Omega_{\boldsymbol{x}}$ moving with a velocity $\boldsymbol{\zeta}$ with respect to the referential domain Ω_χ, the ALE integral formulation of the conservation law (18) becomes for a considered control volume $C(t) \in \Omega_{\boldsymbol{x}}$ (see for instance [22, 19]) :

$$\left.\frac{\partial}{\partial t}\right|_{\boldsymbol{\chi}} \int_{C(t)} u(\boldsymbol{x},t)d\boldsymbol{x} + \int_{C(t)} \nabla.(\boldsymbol{\mathcal{F}}(u_h) - \boldsymbol{\zeta}u) - \int_{C(t)} \nabla.(\nu\nabla u_h) = 0 \tag{26}$$

In two dimensions (respectively 3D) for RD schemes we will take $C(t) = T(t)$ the triangles (respectively tetrahedra) of the mesh $\Omega_{\boldsymbol{x}}$. $C(t)$ and the computation of $\boldsymbol{\zeta}$ has to be chosen such that the Discrete Geometric Conservation Law (DGCL) is respected. The DGCL insures that the resulting numerical scheme should preserve the state of a uniform flow (Farhat *et al* [23]). In practice, DGCL imposes relation between $\int_{C(t)} \nabla.\boldsymbol{\zeta}$ and the temporal discretization used in the scheme. In the present study, the choice $C(t) = T(t) = T^{n+\frac{1}{2}}$ has been made, as proposed by Arpaia *et al*, [19] for advection problem. We give the main steps for the construction of the scheme. The DGCL for the RK2 scheme, is expressed by (for second order case):

$$\int_{T^{n+\frac{1}{2}}} \nabla.\boldsymbol{\zeta} = \frac{|T^{n+1}| - |T^n|}{\Delta t} \tag{27}$$

which gives an explicit nodal expression for the discretization of the mesh velocity :

$$\boldsymbol{\zeta} = \frac{\boldsymbol{x}^{n+1} - \boldsymbol{x}^n}{\Delta t} \tag{28}$$

The idea is to use the stabilized FE analogy to RD scheme (see for instance ([20]) :

$$\sum_{T\ni i}\int_T \omega_i\left(\frac{du_h}{dt} + \mathbf{a}.\nabla u_h + \nabla.(\nu\nabla u_h)\right) = 0 \tag{29}$$

where ω_i the test function is the basis function φ_i going along with a bubble function γ_i : $\omega_i = \varphi_i + \gamma_i$. Let assume the first order approximation u^* corresponding to the first step of the scheme (20) is known.

To get the second order corrected solution, applying the stabilized FE analogy on (26) with the DGCL (27), the galerkin part is written over the ALE conservative formulation :

$$\Phi^{T,Gal} = \int_{T^{n+1}} \varphi_i \frac{u_h^{n+1}}{\Delta t} - \int_{T^n} \varphi_i \frac{u_h^n}{\Delta t} + \int_{T^{n+\frac{1}{2}}} \varphi_i \boldsymbol{\nabla}.\left(\frac{\boldsymbol{\mathcal{F}}(u_h^n)+\boldsymbol{\mathcal{F}}(u_h^*)}{2} - \boldsymbol{\zeta}\frac{u_h^n+u_h^*}{2}\right) - \int_{T^{n+\frac{1}{2}}} \varphi_i \boldsymbol{\nabla}.\left(\nu\boldsymbol{\nabla}\frac{u_h^n+u_h^*}{2}\right)$$

while the stabilization part is written over a non conservative ALE form on the fixed geometry $T^{n+\frac{1}{2}}$:

$$\Phi^{T,stab} = \int_{T^{n+\frac{1}{2}}} \gamma_i \frac{u_h^*-u_h^n}{\Delta t} + \int_{T^{n+\frac{1}{2}}} \gamma_i \left(\boldsymbol{\nabla}.\frac{\boldsymbol{\mathcal{F}}(u_h^n)+\boldsymbol{\mathcal{F}}(u_h^n)}{2} - \boldsymbol{\zeta}.\boldsymbol{\nabla}\frac{u_h^n+u_h^*}{2}\right) - \int_{T^{n+\frac{1}{2}}} \gamma_i \boldsymbol{\nabla}.\left(\nu\boldsymbol{\nabla}\frac{u_h^n+u_h^*}{2}\right)$$

and

$$\sum_{T\ni i}\left(\Phi^{T,Gal}+\Phi^{T,stab}\right)=0 \tag{30}$$

Then, defining

$$\widetilde{\phi_i^T}(u_h) = \int_T \omega_i(\boldsymbol{\nabla}.\boldsymbol{\mathcal{F}} - \boldsymbol{\zeta}\cdot\boldsymbol{\nabla}u_h - \boldsymbol{\nabla}.(\nu\boldsymbol{\nabla}u_h)) \tag{31}$$

which is the nodal fluctuation accounting for the mesh deformation, after some calculations, using mass lumping and DGCL (27), the corrector step (30) writes :

$$|C_i^{n+1}|\frac{u_i^{n+1}-u_i^*}{\Delta t} + \sum_{T\ni i}\left\{\int_{T^{n+\frac{1}{2}}} \omega_i \frac{u_h^{n+1}-u_h^*}{\Delta t} + \frac{1}{2}\left[\widetilde{\phi_i^{T^{n+\frac{1}{2}}}}(u_h^*) + \widetilde{\phi_i^{T^{n+\frac{1}{2}}}}(u_h^n)\right]\right\} = 0 \tag{32}$$

that writes over a RD form ([12, 19]) :

$$|C_i^{n+1}|\frac{u_i^{n+1}-u_i^*}{\Delta t} + \sum_{T\ni i}\left\{\beta_i^T \int_{T^{n+\frac{1}{2}}} \frac{u_h^*-u_h^n}{\Delta t} + \frac{1}{2}\left[\widetilde{\phi_i^{T^{n+\frac{1}{2}}}}(u_h^*) + \widetilde{\phi_i^{T^{n+\frac{1}{2}}}}(u_h^n)\right]\right\} = 0 \tag{33}$$

For the predictor step giving u^*, the exact same reasoning is performed, with an explicit Euler procedure, see Arpaia *et al.* [19], that gives the extension of the RK2 scheme (20) for ALE formulation of advection diffusion equations :

$$\begin{cases} |C_i^{n+1}|\dfrac{u_i^*-u_i^n}{\Delta t} + \displaystyle\sum_{T\ni i}\widetilde{\phi_i^{T^{n+\frac{1}{2}}}}(u_h^n) = 0 \\ |C_i^{n+1}|\dfrac{u_i^{n+1}-u_i^*}{\Delta t} + \displaystyle\sum_{T\ni i}\left(\beta_i^T\int_{T^{n+\frac{1}{2}}}\frac{u_h^*-u_h^n}{\Delta t} + \frac{1}{2}(\widetilde{\phi_i^{T^{n+\frac{1}{2}}}}(u_h^*) + \widetilde{\phi_i^{T^{n+\frac{1}{2}}}}(u_h^n))\right) = 0 \end{cases} \tag{34}$$

5 Numerical results

So as to validate the proposed approach, two simulations are performed. For the two test cases (oscillating cylinder in a fluid at rest and oscillating naca airfoil), the velocity is known analytically and imposed on the solid. The aerodynamical forces are computed to validate the tests but do not intervene in the solid motion.

5.1 Aerodynamical Forces Computations

As just said, the computation of the aerodynamical forces are required. Indeed, in the present study, the motion of the solid is imposed with an analytical function. However, the aim is to be able to perform total FSI problem in which the motion is imposed on the solid *via* external forces such as the aerodynamical ones. Thus, we propose here two computations of those forces.
The first one, that will be quoted in the following by "integral computation" (IC) is performed by interpolating the solution from the simulation on a discretized surface of the solid. Then, the "classical" way of computing the forces is used, by integrating the pressure and the shear stress on the edges of the surface :

$$\mathbf{F}_{IC} = \int_{surface}(-p\underline{\mathbf{I}} + \underline{\pi})\mathbf{n}_{norm}dS \tag{35}$$

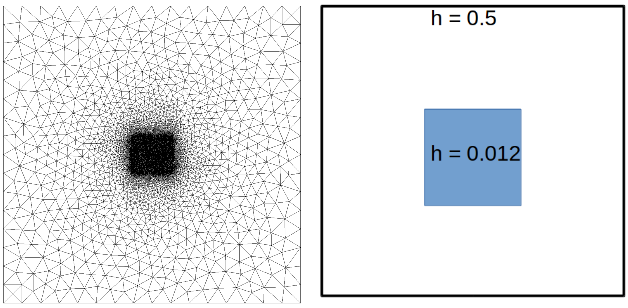

Figure 2: Referential mesh for the oscillating cylinder test case and corresponding sizes

where $\mathbf{n}_{norm}$ is the normalized normal of the solid.
The second approached that will be denoted "change of momentum" (CM) computation from now on, were introduced in [24] and is specific for splitting approach. Before the splitting, the change of momentum $\Delta\mathbf{m}$ inside the solid is computed :

$$\Delta\mathbf{m} = \int_{solid} \rho(\mathbf{u} - \mathbf{u}_S) \tag{36}$$

and the force is :

$$\mathbf{F}_{CM} = \frac{\Delta\mathbf{m}}{\Delta t} \tag{37}$$

This approach presents the advantage to be almost immediate as it is only necessary to evaluate on each penalized element the change of mass before the splitting.

5.2 Inline oscillating cylinder

For this test case, a cylinder ($D = 0.2$) is oscillating in a fluid at rest. The motion is ruled by :

$$x(t) = -Asin(2\pi ft) \tag{38}$$

where A is the amplitude of the oscillation and f its frequency. The dimensionless number characterising this case are the Reynolds number $Re = \frac{U_{max}D}{\nu} = 100$ and the Keulegan-Carpenter number $KC = \frac{2\pi f}{D}$.
The computational domain is $[-10, 10] \times [-8, 8]$ and the referential mesh (13424 vertices and 26782 triangles) is given figure with the sizes used to generate this mesh (2). For the adaptation, the parameter used for the monitor function (10) are : $\beta = 1200$, $\alpha_\psi = 25$, $\alpha_v = 25$, $\gamma = 0.1$, and the physical variable used is the u velocity.
Plot of the velocity and the corresponding adapted mesh are presented figure 3. We can see that the adaptation process allow to have an optimisation of the mesh close to the 0 level set leading to an accurate definition of the solid, and that the mesh adapts well to the physics of the problem.
In order to validate those results, cuts are done at different time and at different position and compared to the literature. The comparison is done with experimental data (Dütsch *et al.* [25]), the Lescape computational code (penalization on structure grids, see Morency *et al.* [24] for the method), and the IBM proposed by Liao *et al.* [26]. The aim here is to show that the combination of unstructured grid/mesh adaptation allow to have competitive results in comparison with structured grids, with a limited number of points. Indeed, the plots show that the present simulation is in good agreement with the literature, but with 13424 vertices compared to the 50000 used in [26] and 1200000 used in the Lescape code (the mesh being uniform in the whole domain).

5.3 Oscillating Naca Airfoil

Flapping wing motions are extensively studied for engineering applications in low Reynolds numbers flow where classical fixed wing geometry performance decreases, [27]. According to previous works, around ten parameters influence the power extraction in flapping wing motions, such as oscillation frequencies and amplitudes (translational and rotational), phase difference between plunge and pitch motion, viscosity, free stream velocity, flapping pattern and airfoil geometry.

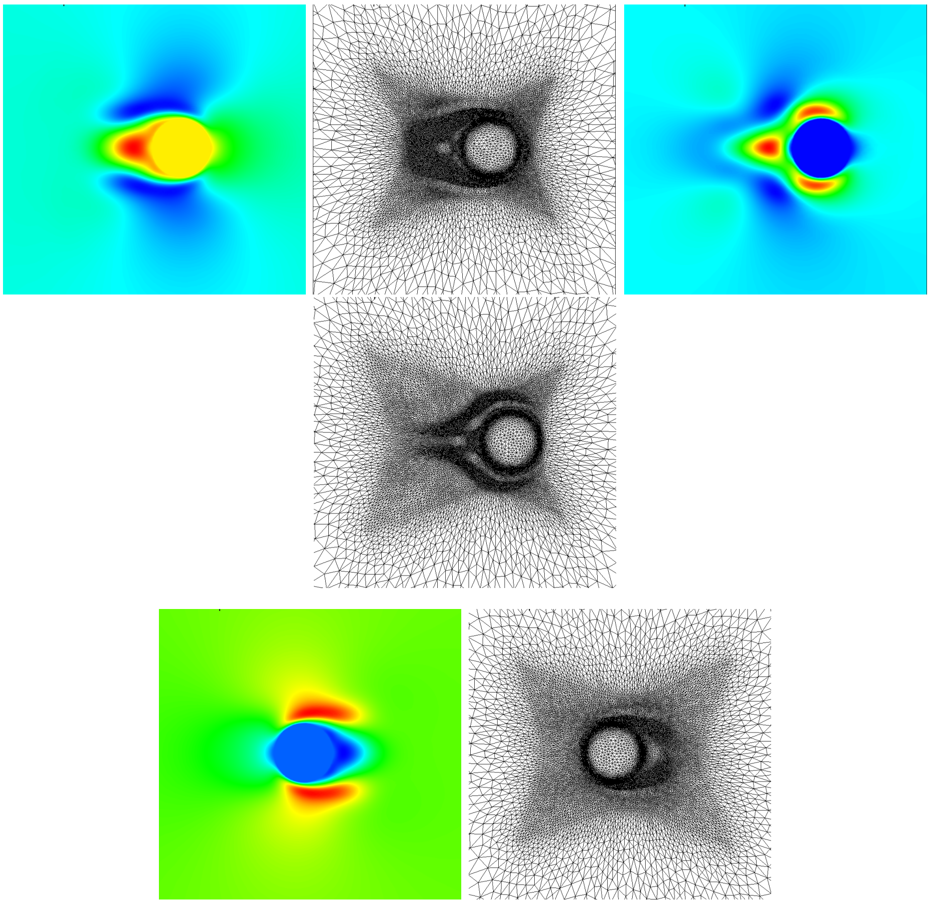

Figure 3: u veloctity and corresponding adapted mesh at different time (zoom close to the adapted area).

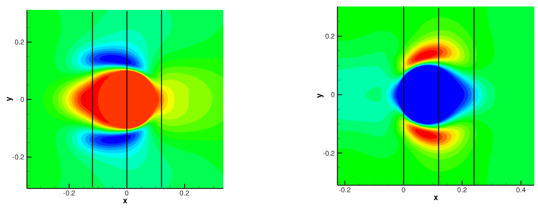

(a) Cuts performed at different times

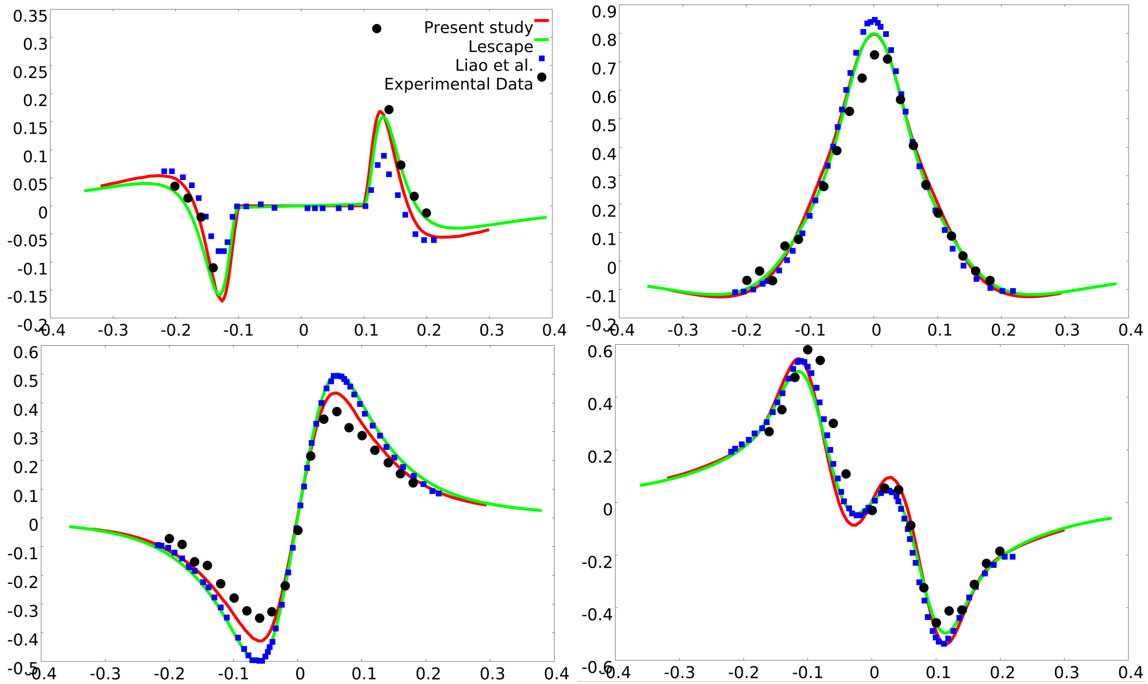

(b) cuts at 180. From top left to bottom right : $x = 0D$, v velocity - $x = 6D$, u velocity - $x = 6D$ v velocity, $x = -6D$ v velocity

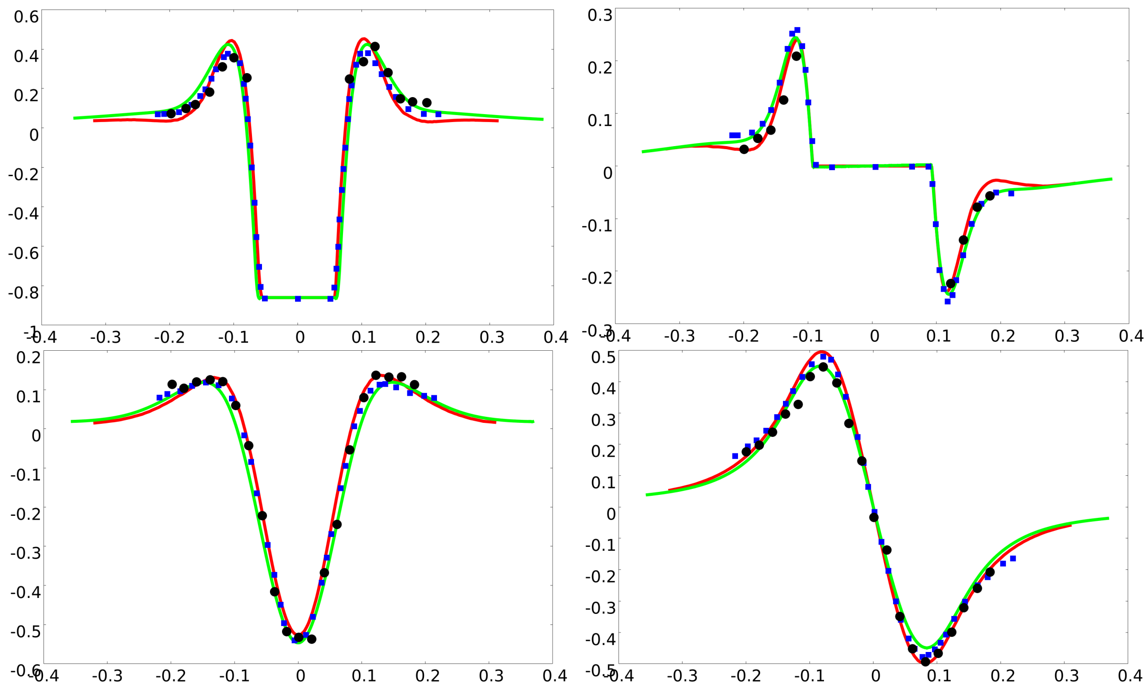

(c) cuts at 330. From top left to bottom right : $x = 0D$, u velocity - $x = 6D$, v velocity - $x = 1.2D$ u velocity, $x = 1.2D$ v velocity

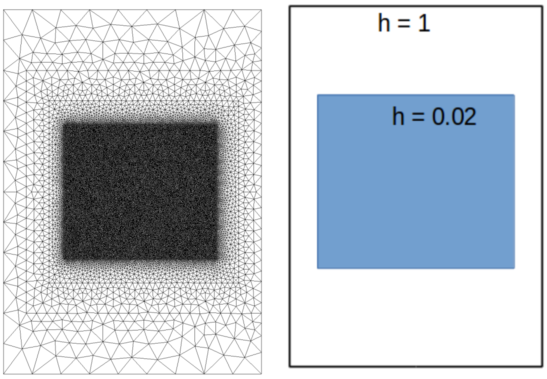

Figure 5: Oscillating Naca test case - Referential mesh

In this section, an oscillating airfoil experiencing simultaneous pitching $\theta(t)$ and heaving $h(t)$ motions is modelled. The infinitely long wing is based on a NACA 0015 airfoil. The pitching axis is located along the airfoil chord at the position $(x_p, y_p) = (1/3, 0)$. The airfoil motion, described by Kinsey and Dumas [28], is defined by the heaving $h(t)$ and the pitching angle $\theta(t)$ as follows

$$\begin{cases} h(t) = H_0 \sin(\omega t + \Phi) \\ \theta(t) = \theta_0 \sin(\omega t) \end{cases} \tag{39}$$

where H_0 is the heaving amplitude and θ_0 is the pitching amplitude. The angular frequency is defined by $\omega = 2\pi f$ and the phase difference Φ is set to 90^o. The heaving velocity is then given by

$$V_y(t) = H_0 \omega \cos(\omega t + \Phi)\,. \tag{40}$$

Based on the imposed motion and on the upstream flow conditions, the airfoil experiences an effective angle of attack $\alpha(t)$ and an effective upstream velocity $V_{eff}(t)$ defined by

$$\begin{cases} \alpha(t) = \arctan(-V_y(t)/U_\infty) - \theta(t) \\ V_{eff}(t) = \sqrt{\left(U_\infty^2 + V_y^2(t)\right)}\,, \end{cases} \tag{41}$$

where the freestream velocity far upstream of the oscillating airfoil is $U_\infty = 68.1$ $(Ma = 0.2)$.

A regime corresponding to the parameters $Re = \dfrac{U_\infty c}{\nu} = 1100$, $H_0/c = 1$, $f = 0.14$, $x_p/c = 1/3$ and $\theta_0 = 76.33^o$ has been computed. The computational domain is of size $[-3, 5.5] \times [-6, 6]$. The finer area in which the adaptation of level set and physics is of size $[-1, 4] \times [-2.2, 2.2]$. It leads to a mesh composed with 30115 vertices and 60186 elements presented with the sizes for the generation on figure 5. For this test case, the monitor function has been slightly modified so as to take into the curvature κ_ψ of the signed distance function :

$$\omega_\psi = \sqrt{\alpha_\psi e^{-\beta\psi^2} + \alpha_\kappa \frac{|\kappa_\psi|}{\gamma_\kappa \max|\kappa_\psi|}} \tag{42}$$

and the coefficient used are : $\beta = 500$, $\alpha_\psi = 22.5$, $\alpha_v = 12.5$, $\gamma = 0.004167$, $\alpha_\psi = 15$, $\gamma_\kappa = 0.36$, the physical adaptation being done according to the vorticity. Figure 6 proposes the vorticity and the corresponding adapted mesh at different times. As for the oscillating cylinder, it is observed that the proposed approach allows to have a refinement close to the solid interface, that imposes accurately the BCs, and that the physics is also precisely resolved in the wanted area thanks to the mesh adaptation. To validate this test case, aerodynamical coefficients are compared to the forces predictions presented by Kinsey et al. [28], by Campobasso et al. [29] and the ones obtained using the Lescape code. The plots can be found on figure 7. It can be seen that the results are in good agreement with the literature. Nevertheless, it is noticed that the CM computation induces an overestimation of the drag coefficient.

6 Conclusion and Future Work

In this work, we proposed a new scheme based on a Strang splitting and ALE RD scheme to solve penalized NS equations. Adaptation conserving mesh connectivity is performed to improve the definition

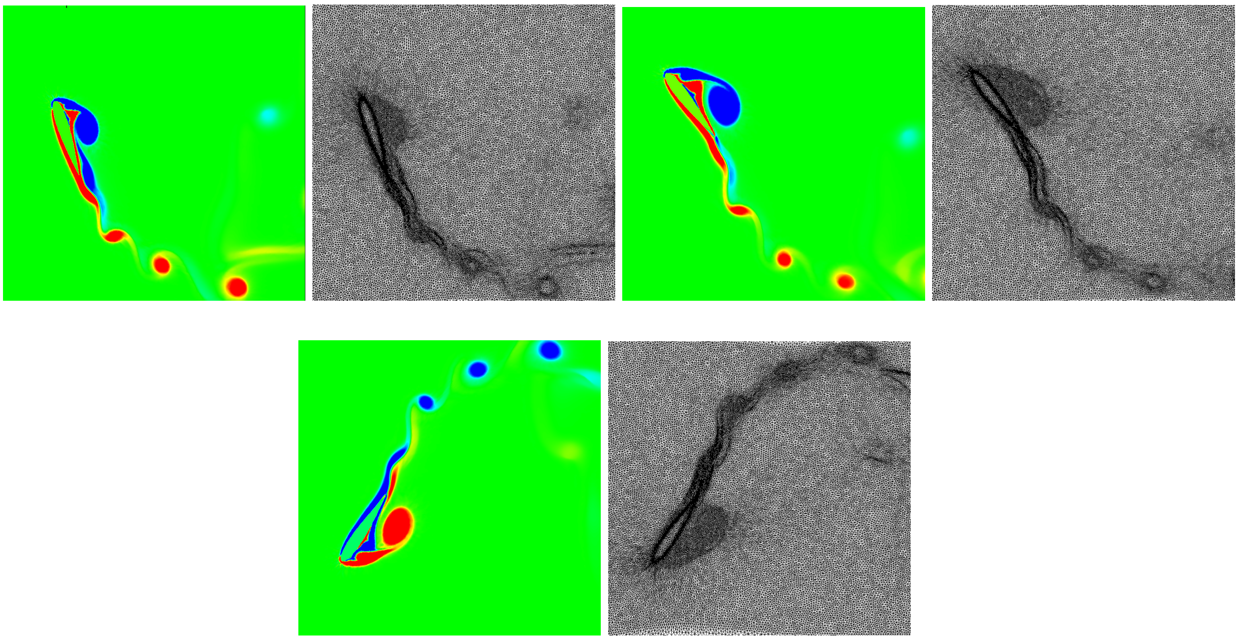

Figure 6: Oscillating naca0015 - Rotational of the velocity and corresponding adapted mesh at different times.

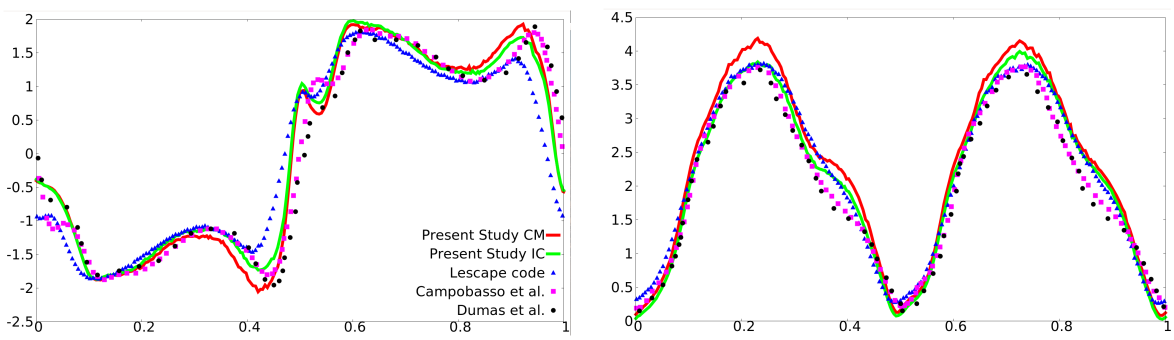

Figure 7: Oscillating Naca0015 airfoil - Aerodynamical coefficients. Left : Lift Coefficient - Right : Drag Coefficient

of solid boundaries. This combination of constant connectivity/ALE schemes presents a real interest when dealing with moving immersed boundaries because remove the constraint of remeshing/interpolation that can be time consuming. The main steps to follow this work will be the use of an implicit time discretization so as to remove the CFL constraint severly restrained by the diffusive aspect of the problem. In addition, even if not discussed here, the question of time consumption of the mesh adaptation strategy needs to be investigated. Indeed, the resolution of the non diagonal linear system by an iterative method represents of course a considerable overhead w.r.t. the CFD, as here the time integration for the flow is purely explicit. By moving to fully implicit procedure the cost of the mesh adaptation will become then negligible compared to the resolution of the nonlinera equations for the flow. From a simulation point of view, the computation of total FSI simulations will be performed (the motion of the solid imposed by the fluid). An interesting and remaining question is the recovery of the accuracy for the BC imposition with the mesh adaptation. Numerical convergence analysis are considered to answer this question.

Acknowledgments

The research leading to these results has received funding from the European Union Seventh Framework Programme FP7/2007-2013 under grant agreement n 605180.

References

[1] H.C. Brinkman. A calculation of the viscous force exerted by a flowing fluid on a dense swarm of particles. *Appl Sci Res*, 1(1):27–34, 1949.

[2] R. Abgrall, H. Beaugendre, and C. Dobrzynski. An immersed boundary method unsing unstructured anisotropic mesh adaptation combined with level-sets and penalization techniques. *J Comput Phys*, 257:83–101, 2014.

[3] G. Strang. On the construction and comparison of difference schemes. *SIAM J Numer Anal*, 5(3):506–517, 1968.

[4] L. Nouveau, H. Beaugendre, C. Dobrzynski, R. Abgrall, and M. Ricchiuto. An adaptive, residual based, splitting approach for the penalized navier stokes equations. *Computer Methods in Applied Mechanics and Engineering*, 303:208 – 230, 2016.

[5] C J. Budd, W Huang, and R D. Russell. Adaptivity with moving grids. *Acta Numerica*, 18:111–241, 5 2009.

[6] Ghina El Jannoun. *Space-Time accurate anisotropic adaptation and stabilized finite element methods for the resolution of unsteady CFD problems.* Theses, Ecole Nationale Supérieure des Mines de Paris, September 2014.

[7] C.H. Zhou and J.Q. Ai. Mesh adaptation for simulation of unsteady flow with moving immersed boundaries. *International Journal for Numerical Methods in Fluids*, 72(4):453–477, 2013.

[8] C. Dapogny and P. Frey. Computation of the signed distance function to a discrete contour on adapted triangulation. *Calcolo*, 49(3):193–219, 2012.

[9] R. Abgrall and P.L. Roe. High order fluctuation schemes on triangular meshes. *J Sci Comput*, 19:0885–7474, 2003.

[10] R. Abgrall. Essentially non-oscillatory residual distribution schemes for hyperbolic problems. *J Comput Phys*, 214(2):773 – 808, 2006.

[11] R. Abgrall, D. De Santis, and M. Ricchiuto. High order preserving residual distribution schemes for advection-diffusion problems on arbitrary grids. *SIAM J Sci Comput*, 36:A955–A983, 2014.

[12] M. Ricchiuto and R. Abgrall. Explicit Runge-Kutta residual distribution schemes for time dependent problems: Second order case. *J Comput Phys*, 229(16):5653 – 5691, 2010.

[13] M. Ricchiuto. *Contributions to the development of residual discretizations for hyperbolic conservation laws with application to shallow water flows.* HDR Thesis, 2011.

[14] P. De Palma, G. Pascazio, G. Rossiello, and M. Napolitano. A second-order-accurate monotone implicit fluctuation splitting scheme for unsteady problems. *Journal of Computational Physics*, 208(1):1 – 33, 2005.

[15] KK Stein, TT Tezduyar, and RR Benney. Mesh moving techniques for fluid-structure interactions with large displacements. *ASME J Appl Mech*, 70(1):58–63, 2003.

[16] H Tang and T Tang. Adaptive mesh methods for one- and two-dimensional hyperbolic conservation laws. *SIAM J. Numer. Anal.*, 41:487–515, 2003.

[17] H. Wang, R. Li, and T. Tang. Efficient computation of dendritic growth with r-adaptive finite element methods. *Journal of Computational Physics*, 227(12):5984 – 6000, 2008.

[18] G. Chen, H. Tang, and P. Zhang. Second-order accurate godunov scheme for multicomponent flows on moving triangular meshes. *Journal of Scientific Computing*, 34(1):64–86, 2008.

[19] L. Arpaia, M. Ricchiuto, and R. Abgrall. An ale formulation for explicit runge–kutta residual distribution. *Journal of Scientific Computing*, 63(2):502–547, 2015.

[20] R. Abgrall and M. Mezine. Construction of second order accurate monotone and stable residual distribution schemes for unsteady flow problems. *Journal of Computational Physics*, 188(1):16 – 55, 2003.

[21] D. De Santis. *Development of a high order residual distribution method for Navier Stokes and RANS equation*. PhD thesis, Univ. of Bordeaux I, 2013.

[22] J. Donea, A. Huerta, J.-Ph. Ponthot, and A. Rodríguez-Ferran. *Encyclopedia of Computational Mechanics*, chapter 14, Arbitrary Lagrangian-Eulerian Methods. John Wiley & Sons, Ltd, 2004.

[23] C. Farhat, P. Geuzaine, and C Grandmont. The discrete geometric conservation law and the non-linear stability of ale schemes for the solution of flow problems on moving grids. *Journal of Computational Physics*, 174(2):669 – 694, 2001.

[24] F. Morency, H. Beaugendre, and F. Gallizio. Aerodynamic force evaluation for ice shedding phenomenon using vortex in cell scheme, penalisation and level set approaches. *Int J Comput Fluid D*, 26:435–450, 2012.

[25] H. Dütsch, F. Durst, S. Becker, and H. Lienhart. Low-reynolds-number flow around an oscillating circular cylinder at low keulegan–carpenter numbers. *Journal of Fluid Mechanics*, 360:249–271, 4 1998.

[26] C.-C. Liao, Y.-W. Chang, C.-A. Lin, and J.M. McDonough. Simulating flows with moving rigid boundary using immersed-boundary method. *Computers & Fluids*, 39(1):152 – 167, 2010.

[27] H. Gopalan and A. Povitsky. Lift enhancement of flapping airfoils by generalized pitching motion. *Journal of Aircraft*, 47(6):1884–1897, 2010.

[28] T. Kinsey and G. Dumas. Parametric study of an oscillating airfoil n a power-extraction regime. *AIAA Journal*, 46(6):543–561, 2008.

[29] M. S. Campobasso and J. Drofelnik. Compressible navier-stokes analysis of an oscillating wing in a power-extraction regime using efficient low-speed preconditioning. *Computers & Fluids*, 67:26–40, 2012.

RESEARCH CENTRE
BORDEAUX – SUD-OUEST

351, Cours de la Libération
Bâtiment A 29
33405 Talence Cedex

Publisher
Inria
Domaine de Voluceau - Rocquencourt
BP 105 - 78153 Le Chesnay Cedex
inria.fr

ISSN 0249-6399